Internet-Based Robotic Laser Scissors and Tweezers Microscopy

ELLIOT L. BOTVINICK[1,2*] AND MICHAEL W. BERNS[1–3]
[1]*Beckman Laser Institute, University of California, Irvine, 1002 Health Sciences Road, East, Irvine, CA 92612*
[2]*Whitaker Institute of Bioengineering, University of California, San Diego, 9500 Gilman Drive, La Jolla, CA 92093-0435*
[3]*Department of Biomedical Engineering, University of California, Irvine, 1002 Health Sciences Road, East, Irvine, CA 92612*

KEY WORDS remote; control; internet; microscope; laser; tweezers; scissors; ablation

ABSTRACT We have engineered a robotic laser ablation and tweezers microscope that can be operated via the internet using most internet accessible devices, including laptops, desktop computers, and personal data assistants (PDAs). The system affords individual investigators the ability to conduct micromanipulation experiments (cell surgery or trapping) from remote locations (i.e., between the US and Australia). This system greatly expands the availability of complex and expensive research technologies via investigator-networking over the internet. It serves as a model for other "internet-friendly" technologies leading to large scale networking and data-sharing between investigators, groups, and institutions on a global scale. The system offers three unique features: (1) the freedom to operate the system from any internet-capable computer, (2) the ability to image, ablate, and/or trap cells and their organelles by "remote-control," and (3) the security and convenience of controlling the system in the laboratory on the user's own personal computer and not on the host machine. Four "proof of principle" experiments were conducted: (1) precise control of microscope movement and live cell visualization, (2) subcellular microsurgery on the microtubule organizing center of live cells viewed under phase contrast and fluorescence microscopy, (3) precise targeting of multiple sites within single red blood cells, and (4) optical trapping of 10 μm diameter polystyrene microspheres. *Microsc. Res. Tech. 68:65–74, 2005.*

INTRODUCTION

The advent of the internet has opened the door to remote computing, remote file sharing, and remote instrumentation control. We have taken advantage of these capabilities to satisfy our need for 24-h access to the laser microscope and to facilitate collaboration and networking with investigators from other locations around the world. The remote operation of microscope systems has been demonstrated for electron microscopes (Chumbley et al., 2002; Hadida-Hassan et al., 1999; Takaoka et al., 2000; Yamada et al., 2003), for light microscope evaluation of fixed samples (Kaplan et al., 2002; Molnar et al., 2003), and for laser scanning confocal microscopy (Youngblom et al., 2001). Though there has been significant progress in developing real-time microscopy and radiological image sharing over the internet, this has not been extended to the domain of real-time interventional manipulation of live cells, tissues, and organelles.

Why would one need 24-h access to the laser microscope? In our case, this is needed to perform delicate subcellular manipulations when individual cells either are at a particular stage in the cell cycle, or need to be manipulated at some point following a previous manipulation (Berns et al., 2000; McNeill and Berns, 1981). Additionally, the needs to follow, to further manipulate, and to gather optical images of either individual or multiple cells after laser manipulation necessitate the development of software–hardware interfaces as well as machine-learning algorithms that allow decision-based operations (Berns and Berns, 1982; Huang and Murphy, 2004; Price et al., 2002).

We have developed a system with remote operational capabilities, using several different standard microscope platforms that have evolved from a multiparametric laser microscope described over two decades ago (Berns et al., 1981). At that time, however, there was neither the computing power nor the internet, two of the key technologies that are combined with current opto-electronic microscopic systems. Development of the "systems-integrated" microscope ("RoboLase") is divided into two distinct subtasks: (1) development of a robotic laser microscope and (2) development of software to share that microscope with other computers on the internet.

MATERIALS AND METHODS

Microscope

The robotic laser microscope is comprised of a motorized inverted microscope stand, external optics to direct the ablation and trapping lasers into the microscope, a CCD digital camera, a hardware–software suite for the control of laser power, the specimen stage, and microscope stand focus and illumination.

The major brands of research microscopes have all developed motorized versions of their inverted micro-

*Correspondence to: Elliot Botvinick, UCSD, SERF 228 MC: 0435, 9500 Gilman Drive, La Jolla, CA 92093-0435, 760-845-6924. E-mail: elliot@ucsd.edu

Contract grant sponsor: The United States Air Force; Contract grant number: AFOSR # F9620-00-1-0371; Contract grant sponsor: The National Institute of Health; Contract grant number: NIH RR 14892.

Received 3 May 2005; accepted in revised form 5 July 2005

DOI 10.1002/jemt.20216

Published online in Wiley InterScience (www.interscience.wiley.com).

scopes. Our system utilizes a Zeiss Axiovert 200M with motorized objective turret, reflector turret (for fluorescent filter cubes), condenser turret, halogen lamp shuttering with intensity control, mercury arc lamp shuttering, camera port selection, objective focus, and parfocality adjustments for switching between objective lenses. The microscope also has a motorized optovar turret to increase the system magnification by 1.6× or 2.5×. For laser ablation experiments, a 63× oil NA 1.4 plan-apochromat PH3 oil objective was used. The microscope stand has a built-in computer, which uses a controller area network (CAN) to communicate with motors and encoders within the microscope stand. The CAN can receive commands through a serial interface typically attached to a computer running an image acquisition/microscope control program. Rather than using the software provided with the microscope, which we found to be cumbersome and slow for our purposes, we have developed custom control software capable of communicating with the CAN as described below.

Features of the motorized microscope which are especially relevant to remote operation of a laser microscope are the shift-free reflector turret, microscope light path selection, illumination control, and objective focus. The shift-free reflector turret allows the user to repeatedly switch between any of five fluorescent filter cubes in the turret without a detectable pixel shift in the image. This is of great importance when performing resolution-limited targeting for laser ablation, as it ensures that the laser will always focus at the expected pixel location. Likewise, the Axiovert microscope can switch between camera ports repeatedly with no detectable pixel shifts when initiating an ablation sequence.

A Zeiss dual video adaptor is mounted on the left hand camera port to allow simultaneous imaging of transmitted light and fluorescence. The 50/50 beam splitter shipped with the video adaptor was replaced with a long-pass dichroic mirror (640 DCLP Chroma Technologies, Rockingham, VT), which passes longer red light and reflects the shorter visible spectrum upwards to the second camera. A band pass filter centered at 680 nm (d680/60× Chroma Technologies) is placed in front of the condenser lens to limit the transmission light wavelengths. Fluorescence emission is reflected upwards by the dichroic mirror into a chromatic image splitter (Dual View, Optical Insights, Albuquerque, NM) that forms two images of the specimen simultaneously on the camera, representing two bands in the visible spectrum. The Dual-View also has a straight-through mode with no image splitting. A closed circuit television camera is mounted on the transmission port of the dual video adaptor for imaging bright field or phase contrast images from the long-red light path. Presently, this camera is not broadcasted through RoboLase, but phase contrast images can be captured with the high-sensitivity camera described later by removing the 680 nm band pass filter.

Specimens are mounted in an X-Y stepper stage (Ludl Electronic Products Hawthorne, NY) controlled with a National Instruments "flexmotion" PXI-7344 stepper motor controller and an MID-7604 power drive (National Instruments, Austin, TX). The flexmotion board is mounted in a PXI computer chassis running the LabVIEW Realtime operating system, which is a graphics-free computing environment designed to maximize performance of control hardware. The RoboLase host computer communicates with the PXI chassis through a local area network (100 Mbps) running TCP/IP protocols. We designed an on-board program to run on the motion controller to allow local joystick control independent of both the host and the PXI computer's CPUs. Motorized objective focus control is achieved through the CAN by Zeiss' Harmonic Drive DC motor, providing 25 nm steps with 10 mm travel for precise focus control over multiple objectives' working distances. To achieve stable temperature control for specimens imaged by an oil-immersion objective lens, both the specimen and the objective lens are heated. Specimens in 35-mm petridishes are heated with a stage heater (heater: DH-35; controller: TC-324B; Warner Instruments Corporation, Hamden, CT) while the objective is heated with a collar-type objective heater (heater: OBJSTD with controller, Bioptechs, Inc., Butler, PA).

The epi-illumination system was removed from the microscope stand for direct access by the trapping beam to the back aperture of the microscope objective. The epi-illumination system was mounted distal to the microscope and coupled through two 400 mm positive achromatic doublets (Newport Corp., Newport, CA) into the microscope. The motorized Axiovert ships with a motorized shutter for the fluorescence light path which we removed because of inherent delays between computer commands to open the shutter and the opening event. Instead, an electronic shutter (Vincent Associates, Rochester, NY) was mounted between the arc lamp and the epi-fluorescence lens system, with a notable decrease in delay time.

Connectivity of key controllers and actuators in RoboLase is demonstrated in Figure 4. The unique identifiers in each block of the diagram (e.g., 610C) are for reference to an online reference manual available at http://robolase.ucsd.edu. The Main PC, which runs the RoboLase software, connects to the ablation laser and the microscope through two serial communications: to the ORCA camera controller through a firewire connection and to a PXI chassis through the RoboLase local network. The PXI chassis contains a motion control card that connects to a stepper motor driver that responds to joystick commands, controls two shutter drivers, and drives the XY microscope stage. The chassis also contains a data acquisition card that receives data from a power meter and communicates with the ablation laser's beam steering controller through analog voltage outputs.

External Laser Optics and Hardware

Optics outside the microscope stand guide the ablation and trapping lasers into the microscope and supplies RoboLase with automated laser power control, laser shuttering, and laser power monitoring (Fig. 1). The laser ablation light source is a diode-pumped Spectra-Physics Vanguard with a second harmonic generator (SHG) providing TEM_{00} mode 532 nm laser light linearly polarized with 100:1 purity with a 76 MHz repetition rate, 12 ps pulse duration, and 2 W average power. The unattenuated laser power is far in excess of that necessary for resolution-limited subcellular laser ablation (Botvinick et al., 2004) and left unattenuated

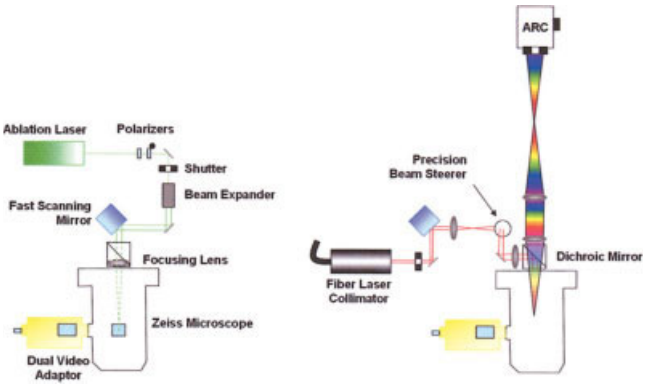

Fig. 1. External laser light paths. The left panel shows the light path of the ablation laser (in green). The laser beam passes through a shutter, is expanded, and directed onto a fast scanning mirror for beam steering. The steered beam is directed to the Keller camera port underneath the microscope where a mirror reflects the beam up through the microscope stand and into the microscope objective. The right panel shows the light path of the trapping laser (in red) and the externalized epi-fluorescence light path (rainbow). The laser beam is expanded by two biconvex lenses and mixed with the arc lamp light with a short pass dichroic mirror. Custom dichroic mirrors in filter cubes housed in the microscope's reflector turret reflect the laser and part of the arc lamp's visible spectrum up into the microscope objective.

is well above the plasma threshold causing catastrophic damage to cells in the vicinity of the laser. We built a beam attenuator from dual linear polarizers. The laser beam polarization purity is considerably increased from 100:1 through the first glan linear polarizer (CLPA-12.0-425-675, CVI Laser, LLC, Albuquerque, NM) with a 5×10^5 extinction ratio rotated for maximum transmission (95%). Laser power is controlled by rotating an identical glan linear polarizer placed in series to the first and mounted in a motorized rotational mount driven by an open loop 2-phase stepper motor with 0.05° accuracy (PR50PP, Newport Corp.). The stepper motor rotates the polarizer from its vertical orientation with maximum transmission (95%) to its horizontal orientation with minimum transmission well below the damage threshold of biological samples. The stepper motor is controlled via the flexmotion board in the PXI chassis. Light exiting the second polarizer is partially reflected by a laser-line beam sampler, with dual antireflection-coated surfaces. The sampled beam is measured by a photodiode (2032 photoreceiver, NewFocus, San Jose, CA) and converted to a voltage. A calibrated photometer (1825-C, Newport Corp.) is used to determine the relationship between the photodiode voltage and average laser power in the main beam. A mechanical shutter (Vincent Assosiates) with a 3-ms duty cycle gates the main laser beam to provide "short" bursts of pulses to the microscope.

The laser beam is then expanded using an adjustable-beam expander (2–8×, 633/780/803 nm correction, Rodenstock, Germany) and lowered to a height just above the optical table by two additional mirrors. Telecentric beam steering is achieved by placing a single dual-axis fast scanning mirror (Newport Corp.) at an image plane conjugate to the back focal plane of the microscope objectives. This image plane is formed by a 250 mm biconvex lens positioned with its front focal plane at the image plane of the microscope Keller port (below the microscope stand) and with its back focal plane at the fast scanning mirror surface. To access the submicroscope Keller port, the microscope is raised 70 mm above the table via custom-machined metal alloy posts to leave room for a 45° mirror, which vertically redirects incident laser light running parallel to the table through the Keller port (Fig. 2). Once inside the microscope stand, the laser light passes through the tube lens and one of the five fluorescent filter cubes of the reflector turret before entering the back of the objective lens. The reflector turret can be set up either with one filter slot blank or since the turret is automated, the system can position a fluorescent filter cube into place, with appropriate laser transmission characteristics. All external mirrors in the ablation laser light path are virtually loss-less dielectric mirrors optimized for 45° reflections of 532 nm S-polarized light (Y2-1025-45-S, CVI Laser LLC, Albuquerque, NM).

The trapping laser light source is an Ytterbium continuous wave fiber laser with a 5-mm collimator providing randomly polarized TEM_{00} mode 1,064 nm laser output with 10 W maximum power (IPG Photonics Corp., Oxford, MA). Laser power is controlled programmatically through serial port communication. Laser light is reflected off two mirrors and into a custom beam expander comprised of two anti-reflection coated bi-convex lenses (f = 100 mm, 400 mm) placed telescopically to expand and collimate the beam. The 100 mm lens is placed so that its back focal plane lies on the surface of the second mirror, which is mounted in a second dual-axis fast scanning mirror (Newport Corp.) to achieve telecentric beam steering in the specimen plane. The laser then reflects off a 2 inch diameter short pass dichroic beam splitter placed behind the microscope in the arc lamp illumination light path to merge the two light paths. Laser light is then reflected upwards by a dichroic mirror mounted in the reflector turret, and into the back of the objective lens where it is focused in the specimen plane. The 100 mm lens mount can be adjusted axially to move the laser trap depth relative to the image plane. A mechanical shutter is placed in the beam path and is controlled by the flexmotion controller. All external mirrors in the trapping laser light path are virtually loss-less dielectric mirrors optimized for 45° reflections of 1,064 nm S-polarized light (Y1-1025-45-S, CVI Laser).

Cameras

A high quantum efficiency digital camera is used to capture transmitted and fluorescent images. RoboLase implements a Hamamatsu Orca-AG deep-cooled 1,344 × 1,024 pixel 12-bit digital CCD camera with digital (fire wire) output. The ORCA can read out sub regions of the chip for increased frame rates, bin pixels for increased signal-to-noise, and adjust gain and exposure time to trade off between signal-to-noise characteristics and arc lamp exposure times. RoboLase uses Hamamatsu's Video Capture Library for LabVIEW (ver 1.0) plug-in to communicate with the ORCA camera controller through its DCAMAPI driver (Fig. 3).

Software

Two pieces of software are engaged during operation of the RoboLase microscope. The first is the hardware

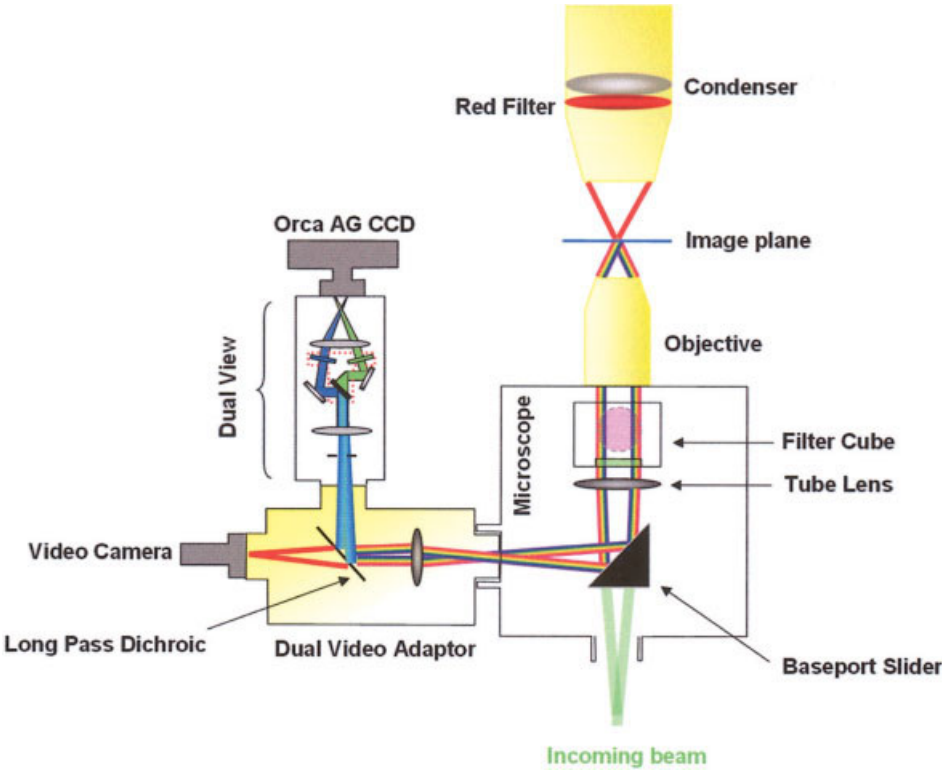

Fig. 2. Internal light paths. Optics were chosen to passively mix and separate visible and NIR light. Green laser light enters from underneath the microscope stand through the Keller port, the tube lens, one of the reflector turret's filter cubes, and the microscope objective. NIR light from the trapping laser and visible light from the arc lamp (both shown as purple circle in the filter cube) enter the back of the microscope stand, normal to the plane of this figure, and are reflected upwards by one of the reflector turret's filter cubes. Long-red light from the halogen lamp is selected by a filter in front of the condenser for phase contrast imaging. Visible emission from the specimen enters a dual video adaptor modified to pass the long-red phase contrast light to the video camera and to reflect the shorter wavelength fluorescent emission up through the dual view system and onto the ORCA-AG CCD camera.

control suite, and the second is the web server responsible for sharing RoboLase with remote users. The control software programmed in the LabVIEW 7.1 (National Instruments) programming language is responsible for control of the microscope, cameras, and external light paths. The control software also manages image and measurement file storage. It communicates with the user through the graphical user interface or the "control panel" in LabVIEW. The control panel receives user input and displays images and measurements. The control software interprets commands sent by the user into appropriate hardware calls and returns the results of that action to the front panel and/or computer's hard drive. Emphasis was placed on the design of the front panel, such that it would be easy to learn while providing the features needed to search for a cell of interest and then to perform cellular manipulation on that cell.

Figure 4 shows a snapshot of the front panel. The upper-left panel contains laser parameter controls. This panel contains two tabs: one in green to control the ablation laser and one in blue to control the trapping laser. Ablation laser controls include a slider to select power in the focal plane, two buttons to fire the laser either at the center of the field or at the green crosshairs which are positioned with the mouse, and selection of the filter cube turret position during ablation. Once either fire button is pressed, the control software calls the microscope CAN to select the Keller port and the appropriate filter cube. The control software then continuously quarries the CAN to ensure the completion of both actions before opening the shutter for a single 3 ms laser burst. Beam steering is sufficiently faster than the camera port and filter turrets, such that a quarry of its position prior to opening the shutter is unnecessary. Laser tweezers controls (not shown) include laser power selection, shutter state and beam positioning controls.

The center panel on the left contains stage and ablation laser steering controls. The "stage control" tab contains left/right and up/down rockers to move the microscope stage with position feedback. A slider selects either step or servo mode to move the stage either in increments specified in the "X/Y Step Size" control, or continuously while the rockers are pressed. A similar pair of rockers moves the microscope objective for focus control. The "Click and Move" control is a novel control designed to minimize exposure of the cells to the arc lamp light during stage movements. The user simply chooses the crosshair tool from the toolbar to the left of the image and clicks on an object of interest in the image. The program then calculates that pixel's displacement from the field of view center and moves the stage to center the object. The "Expose?" check box provides the option to follow the move with an exposure. The "Coordinate List" tab allows the user to store the current position in a list or to return to any stored coordinate. The "Coordinate Utility" tab allows the user to load an old list of coordinates, to clear the current list, or to save the current list to the hard drive. The "Special Moves" tab contains controls for beam steering and for laser ablation through a series of z-coordinates. The user can select the rectangle tool from the tool bar and draw a rectangle around a region in the image. There is a control in this tab to carve out that rectangle by firing single macropulses (one opening of the mechanical shutter which will pass multiple individual laser pulses) at evenly spaced locations in the rectangle. Since the laser causes near diffraction-limited ablation

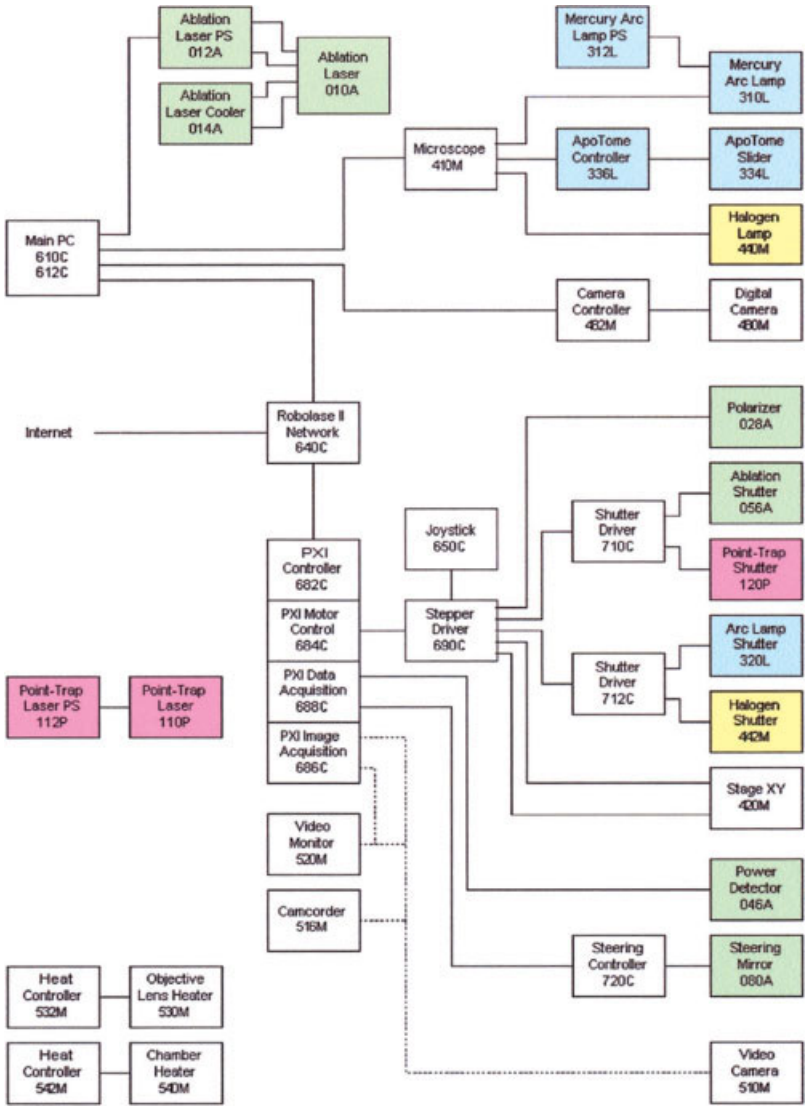

Fig. 3. RoboLase hardware map. The figure diagrams connectivity between RoboLase hardware.

(Botvinick et al., 2004), the program calculates the number of macropulses necessary to fill in the rectangle based on the pixel dimensions of the rectangle and the pixel extent of a single diffraction-limited ablation.

The lower panel on the left contains image acquisition controls. The "Image Acquisition" tab contains controls for exposing single images, continuous acquisition (Focus), image storage, and image printing. The user can select the filter cube to place during the acquisition, whether to gate the arc lamp during the exposure, and controls to calculate a ratio image when used with the chromatic image. The "Root Directory" control specifies the top directory for file saving using our automated file naming system, and an indicator displaying the full path and name of the last saved image. The file path and name are designed to prevent accidental overwriting of data during successive operations of the program, coding the file name with the current time. The "Time Series" tab contains controls for acquiring a time series of images. The time series uses setting from the "Image Acquisition" tab and contains controls for the number of images and the duration between images as well as an indicator of the last image saved in the time series. The "Raster Scan" tab has a control to raster through user-selected stage coordinates and acquire images at those locations at time durations set through a control.

The lower panel on the right contains camera and microscope controls. The "Image Display" tab displays the last acquired image plus the toolbar for selecting ablation and click-and-move coordinates. The "Microscope Control" tab contains controls for the microscope stand to select the objective, filter cube, condenser filter, optovar, and image port. The "Camera Controls" tab contains controls for camera gain, digitization offset, exposure time, and binning. It also contains an area-of-interest control to only transfer image data from an area of interest defined with the rectangle tool in the image display. Lastly, this tab has controls for click and move parameters including pixel coordinates of the field of view center and the pixel/microscope step gain.

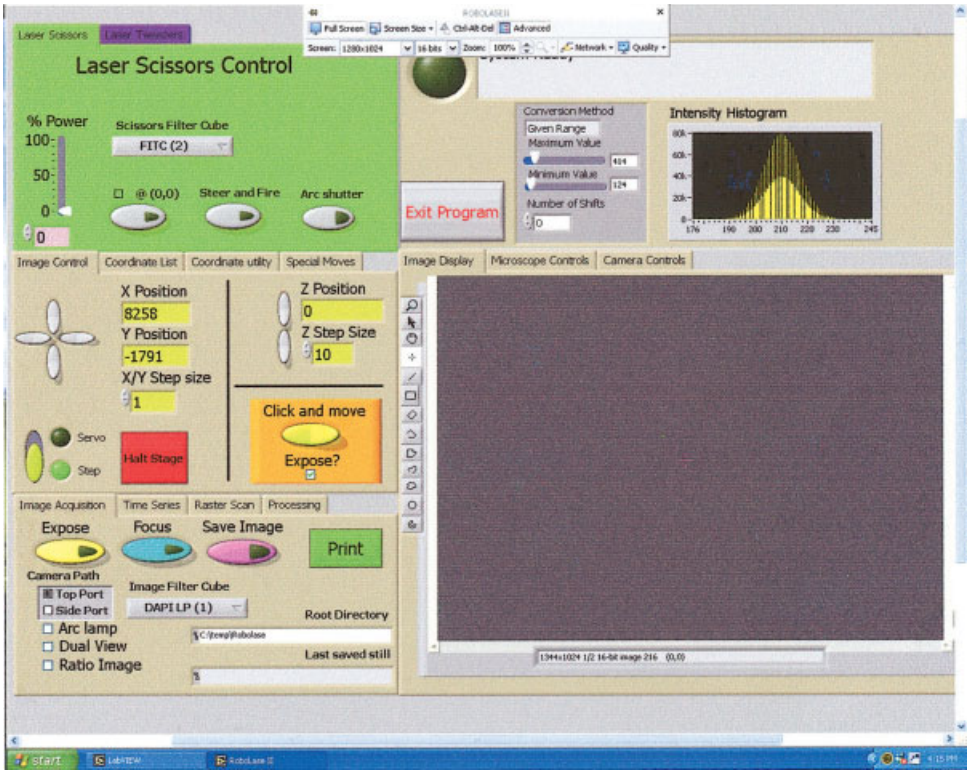

Fig. 4. RoboLase control panel. The control panel as viewed during a logmein.com session. The gray box at the top of the screenshot is a drop-down menu to configure the logmein.com session during operation. Shown are controls for stage movement, laser ablation, and image acquisition/display. The intensity histogram of each image is displayed to aid in determining the proper setting for camera acquisition and image display.

The upper panel on the right contains a message box and the image histogram. The message box displays important messages, such as error notifications or equipment status, and draws user attention by pulsing the large green digital LED to the left of the message box when a new message arrives. The gray box controls the image display lookup table for mapping 12-bit images to the 8-bit display. This control uses four modes of look-up table: (1) Full-dynamic, in which the range of nonzero intensities are divided into 256 equally spaced bins, (2) 90%-dynamic, in which the dynamic range containing the middle 90% of the cumulated histogram of the image is divided into 256 equally spaced bins, (3) Given-range, in which the range of grayscale values specified by the "Maximum Value" and "Minimum Value" slider controls are equally divided into 256 bins, and (4) Down-shift, in which the grayscale values are shifted to the right in 8-bit increments, as specified by a control. An image histogram displays the pixel intensity histogram of the last acquired image to aid in the selection of an appropriate lookup table and to quantify separation between the background noise mode and the pixels of interest.

Web Server

Two web server packages were compared. The first is the "remote panel" feature provided by National Instruments as a feature of LabVIEW. The LabVIEW web server publishes the control panel as an html document to which multiple users can log on during runtime. Once users connect to the RoboLase webpage, the front panel of RoboLase will appear in their web browser window with all the functionality available to a user operating from the host computer. Those logged on can either participate as an observer, or request control of the control panel to perform an experiment. It is not necessary for the remote user to have LabVIEW installed. To operate the RoboLase remote panel, it is only necessary to install the free LabVIEW run-time engine installed automatically at the first connection to any remote panel. The server can be configured to allow browser access for viewing, viewing and controlling, or to deny access to a programmable list of IP address. The LabVIEW protocol works by only transmitting changes to the control panel as they occur, as opposed to continuously transmitting the entire control panel as well as the states of the buttons and controls.

The second webserver is a web-based protocol "Log me in" available at www.logmein.com (3am Labs, Inc., Woburn, MA). Logmein.com belongs to a family of software that allows remote control of a PC through a live window that functionally duplicates the host PC from anywhere with an Internet connection. Logmein.com uses a peer-to-peer session handoff to provide high-speed remote control by eliminating the gateway, thereby allowing the two PCs to communicate directly. The logmein.com host computer (RoboLase) maintains a constant secure sockets layer (SSL)-secured connection with one of the logmein.com gateways. This link is initiated by RoboLase and the firewall treats it as an outgoing connection. The client browser operated by a remote user establishes a connection to Logmein.com and authenticates itself after which the gateway forwards the subsequent encrypted traffic between the client and the host. The remote user is not required to download additional programs to connect to RoboLase; however, there is an optional ActiveX control download to improve image quality. The user can switch the host's display between "low quality" 8-bit color images

and "high quality" 16-bit color images during the session to trade off between color resolution and frame transfer rates.

RESULTS (SYSTEM OPERATION)

Time delays between commands received on the host computer and the completion of actuation were characterized by programmatically placing timers in the RoboLase control software. Time delays during switching between ablation and imaging were maximized during measurement by imaging through the binocular port with filter cube 2 and ablating from the Keller port through filter cube 5. When switching from imaging to ablation, the system takes 610, 19, and 20 ms (mean, standard deviation, and N) for the imaging port transition and 688, 6, and 10 ms for the filter cube transition, with a total duration of 1400, 41, and 10 ms from the press of the button to the completion of the ablation, with a 3 ms laser exposure time. A two tailed t-test showed no significant increase in total ablation time when the laser is steered before the ablation ($P > 0.05$, $N = 10$ for both samples). The imaging port transition required switching both the baseport slider and the side port turret. When switching from ablation to imaging, the system takes a total 1387, 103, and 10 ms to transition the imaging port and the filter wheel followed by 677, 34, and 10 ms or 702, 34, and 10 ms for the subsequent image with or without operating the arc lamp shutter, respectively. The images were acquired in snap mode with a 1 ms exposure time to measure the latency of the camera digitization and readout. Computational latency during continuous image acquisition was quantified by measuring the total time to acquire a set of images (1 ms exposure time each) in which the size of the sets ranged from 23 to 36 individual images. The total times of ten sets were recorded and averaged within the sets with a between-set average 133, 3, and 10 ms per image delay time.

Four proof of concept experiments were conducted to demonstrate internet control of Robolase. The first proof of concept experiment was between San Diego, California, USA and Miami, Florida, USA using a hotel administered T1 connection operating at a maximum of 10 Mbps. This experiment tested remote control of the microscope stage movement and control of objective focus (Fig. 5). High resolution images were acquired with a 63× PH3 phase contrast NA1.4 oil immersion objective. This experiment implemented the LabVIEW web server for remote operation. Note the resolution of the double-membrane nuclear envelope. Images transfer times were 2–3 s per image for a 256 × 256 subregion of the CCD.

The second experiment was conducted from Miami, Florida (USA), again implementing the LabVIEW web server. In this experiment, cells with green fluorescent protein labeled microtubules were observed and manipulated under phase contrast and epi-fluorescence illumination (Fig. 6). In these cells, the centrosome microtubule organizing center (MTOC) was irradiated with the laser scissors (Botvinick et al., 2004). The MTOC region was irradiated at three different time points, with a progressive loss of fluorescence with each laser exposure. In this experiment, the following remote procedures occurred: (1) the microscope stage was moved until an appropriate cell was located, (2) the microscope was focused at different z-axis optical planes in the cells to determine the desired optical plane for laser exposure, (3) laser parameters (wavelength, power/energy, and number of exposures) were selected, (4) the laser was targeted to a specific region (the MOTC) in the cell, and (5) the result was digitally recorded and the cell was followed for a desired time period. In this particular cell, two laser exposures were performed until the desired ablation was observed.

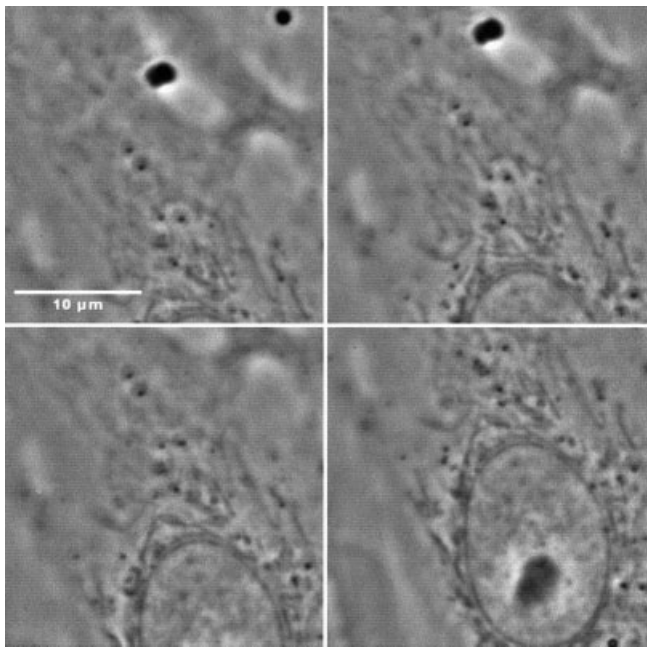

Fig. 5. A remote session from Miami, Florida, USA in which PTK2 cells were imaged with a 63× PH3 oil immersion objective. The experimenter remotely adjusted the camera gain, acquisition time, and region of interest to optimize contrast and reduce image data size. Subfigure panels demonstrate remote operation of the X–Y stage and objective focus during a remote experiment. Note resolution of the double membrane nuclear envelope.

The third experiment, which was conducted from Brisbane, Queensland, Australia implemented the Logmein.com web server. In this experiment beam steering for remote laser targeting and ablation over a long-distance internet connection was demonstrated (Fig. 7). Red blood cells were deposited on a microscope cover glass by the smear method and mounted in a rose chamber (Berns et al., 2005). Remote control of the system from Australia successfully demonstrated (1) all of the manipulation capabilities described in the previous experiment, (2) that the ablation laser beam could be moved to different locations in the same cell, with a spatial resolution of less than a micron for both the lesion diameter as well as the distance between individual lesions, and (3) that multiple discrete visible lesions could be placed in the same cell. The time from initial remote command (pressing of the fire button) in Australia to actual observation of the event on the host RoboLase system was determined by measuring delay times between oral communication of the command over a telephone connection and actuation of the command on RoboLase. Any delay time was unperceivable.

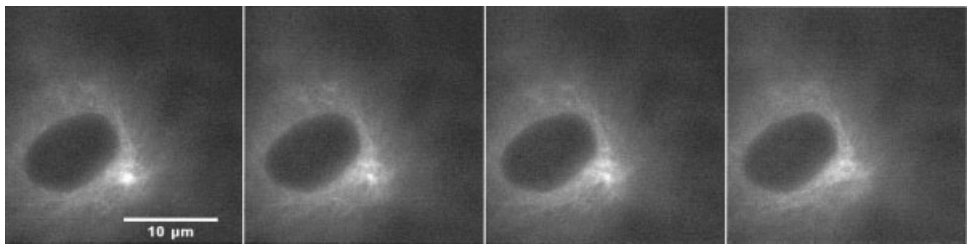

Fig. 6. A remote session from Miami, Florida, USA demonstrating remote fluorescence-guided subcellular surgery. The remote user searched for an appropriate cell and interactively focused and positioned the microtubule organizing center (procedure not shown) below the laser scissors crosshair (first image). The next images show: postfiring of 3 ms macropulse, the remaining region of the microtubule organizing center interactively positioned below the laser scissors crosshair, and a second 3 ms macropulse fired to delete the remaining microtubule organizing center.

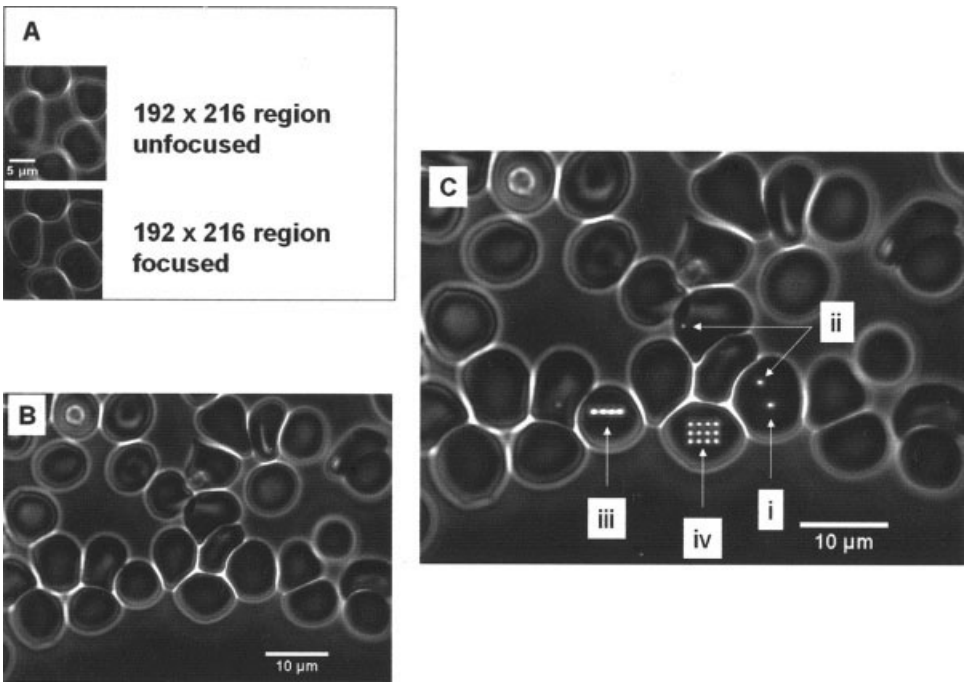

Fig. 7. Two remote sessions from Brisbane, Queensland, Australia demonstrating remote laser ablation in phase contrast. Dried and smeared erythrocytes serve as a convenient test specimen and targeting guide. **A**: In the first session, the remote user selected a region of interest of the CCD chip to speed image transfer for focusing the specimen. Shown is pre and postfocusing. **B**: In the second session, a region of cells was brought into focus remotely. **C**: The remote user demonstrated RoboLase's beam steering capabilities by ablating at the center of the field under the purple crosshairs shown in figure 4 (i), ablating single shots by beam steering (ii), ablating along a line (iii), and ablating within a remote user-defined rectangle (iv). For cases iii and iv, the user defined the pixel radius of a single ablation, and RoboLase calculated the number of laser exposures necessary to fill the region in. For illustration, we have purposefully increased this number to delineate individual ablations within the region.

Full-frame transfer rates were measured by counting the number of screen refreshes per 10 s interval. An 8.2 frames/s rate measured from the RoboLase host computer corresponded to 1.5 frames/s in low quality mode and 0.7 frames/s in high quality mode.

The fourth experiment, conducted from Atlanta, Georgia, implemented the Logmein.com web server. In this experiment, 10 μm diameter DNA-Check fluorospheres (Coulter Corp., Hialeah, FL) were suspended in water in a 35 mm glass-bottom Petridish in which thermal flow in the water was induced by heating the objective lens using the objective heater set at 37°C. The remote user selected "focus" mode on the control panel to stream images across the internet. The remote user was able to open and close a mechanical shutter, allowing the trapping beam to be focused on the target microsphere through a push-button control in the laser tweezers tab of the control panel. A time series was recorded after a microsphere was trapped and then released to demonstrate the ability of a remote user to manipulate objects with the laser tweezers (Fig. 8). A 40× oil 1.3NA PHIII objective lens was used.

DISCUSSION

We have engineered a robotic laser scissors and tweezers microscope that can be operated via the internet using most internet accessible devices including laptops, desktop computers, and personal data assistants (PDAs). The system affords investigators the ability to conduct micromanipulation experiments (cell surgery or trapping) from remote locations (i.e., between the US and Australia). This system greatly expands the availability of complex and expensive research technologies via investigators networking over the internet. It serves as a model for other "internet-friendly" technologies leading to large-scale networking and data-sharing between investigators, groups, and institutions on a global scale. The system offers three unique features: (1) the freedom to operate the system from any internet capable computer, (2) the ability to image, ablate, and/or trap cells and their organelles by "remote-control," and (3) the

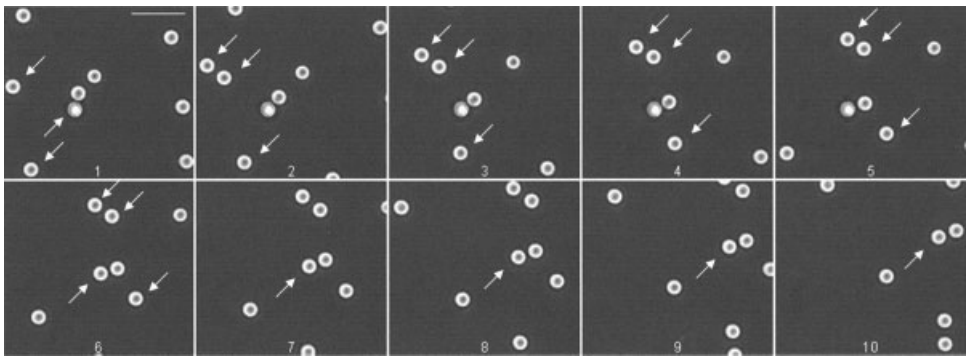

Fig. 8. A remote session from Atlanta, Georgia, USA in which 10 micron diameter microspheres were remotely captured in the laser tweezers. Every fifth frame of an 8.2 frame/sec time series is shown. In frame 1, the two downward-left arrows (three arrows in subsequent frames) indicate reference microspheres moving through fluid flow in a 35-mm petridish. The upward-right arrow indicates a microsphere captured in the laser tweezers. A slight axial displacement of this microsphere (due to the laser tweezers) as compared with the free-floating microspheres can be observed, as the center dark region of the microsphere has transitioned to white. Frames 2–5 show the displacement of the reference microspheres relative to the "trapped" microsphere. Just prior to frames 6–10, the remote user released the microsphere from the trap through a RoboLase control (note the reversal of the axial displacement), and the microsphere is carried away by the fluid flow. Notice the second microsphere attracted to the laser focus but held away by the trapped one.

security of operating the system in house from the researcher's own laptop without the risk of leaving data on the host computer. Four "proof of principle" experiments were conducted: (1) precise control of microscope movement and live cell visualization, (2) subcellular microsurgery on the microtubule organizing center of live cells viewed under phase contrast and fluorescence microscopy, (3) precise targeting of multiple sites within single red blood cells, and (4) laser trapping of an individual cell.

RoboLase should be applicable in a wide array of live cell experiments. However, there may be some limitation in a true real-time experiment. Although the high-speed beam steering by the Fast Scanning Mirrors is a low-cost solution to large time delays of microscope-stage targeting, there is still a net dead-time of nearly three and one-half seconds between the "computer-click" of ablation and the display of the next image (however image acquisition can begin after about 2 and one-half seconds). Ideally, the ablation laser's wavelength would be tunable allowing entry of the laser through the fluorescence excitation light path, regardless of the fluorescent filter cube excitation band. Given our fixed wavelength, we decided the simplest solution would be to utilize the Keller port and the motorized turret. This limitation could be minimized in future designs of the instrument by employing a tunable laser system. The ablation laser wavelength (532 nm) used in our current system design belongs to the excitation band of many common fluorophores, including GFP, YFP, and FITC so that ablation would only require changing the imaging path and not the reflector position. In this case, image acquisition could begin about one and one-half seconds after the computer click. Researchers studying changes immediately following the ablation (in the first 4 s), for example cytoskeletal dynamics, could interface the ablation laser into the epi-fluorescent light path. RoboLase described here, however, is similar in specification to a laser system used to ablate single cytoplasmic microtubules and to follow the subsequent depolymerization of the irradiated microtubules (Botvinick et al., 2004).

We also tried two web servers to remotely control RoboLase. The National Instruments web server transmitted single commands reflecting changes in the state of buttons and controls from the control panel, with no significant delay by human standards. Image transfer, however, took seconds even when transmitting small regions of interest. It is a known issue at National Instruments that embedding images into the front panel significantly slows the execution of the program. On several occasions, the long delay times during image transfer concurrent with over-zealous clicking of control buttons lead to a system crash. Our conclusions are that while the remote panel and web server built into LabVIEW are well suited for nonimaging applications, the system performs poorly for RoboLase. The LabVIEW programming language, however, has proven to be robust and stable enough to build our control application. The logmein.com service significantly outperformed LabVIEW's. Transfer rates were faster by seconds and it did not require a download and installation, such as LabVIEW Runtime. One key advantage to the LabVIEW server is the ability to connect to multiple users at once. Since the key goals of this project were to make RoboLase available to teaching and multi-site collaboration, the utility of logmein.com is limited unless the collaboration only consists of one researcher on the host computer and one remote researcher. As technologies for computer sharing evolve, there is little doubt that systems such as RoboLase will become ubiquitous in the research community, as they lend themselves to the growing culture of international collaboration and globalization of science.

ACKNOWLEDGMENTS

Dr. Botvinick thanks the Arnold and Mabel Beckman Foundation's Beckman Fellow's program for supporting his research. We give special thanks to David Little for helping develop the code for the first generation of RoboLase, and for his help with optical alignment and supporting hardware communication as well as documenting the current project. We all give special thanks

to our graduate students Jaclyn Vinson and Adrian Mei and to our postdoctoral researcher Linda Shi for helping with optical light path design, beam alignment, hardware control, and upkeep of the RoboLase system. We also thank Halina Rubensztein-Dunlop and her laboratory at the University of Queensland Australia, and Gregory Berns at Emory University for participating as "remote" users in the online proof of concept experiments. Recognition is also given to Drs. Zifu Wang and Joon You of the University of California, Irvine for their contributions to the early iteration of the RoboLase system.

REFERENCES

Berns GS, Berns MW. 1982. Computer-based tracking of living cells. Exp Cell Res 142:103–109.

Berns MW, Aist J, Edwards J, Strahs K, Girton J, McNeill P, Rattner JB, Kitzes M, Hammer-Wilson M, Liaw LH, Siemens A, Koonce M, Peterson S, Brenner S, Burt J, Walter R, Bryant PJ, van Dyk D, Coulombe J, Cahill T, Berns GS. 1981. Laser microsurgery in cell and developmental biology. Science 213:505–513.

Berns MW, Wang Z, Dunn A, Wallace V, Venugopalan V. 2000. Gene inactivation by multiphoton-targeted photochemistry. Proc Natl Acad Sci USA 97:9504–9507.

Berns MW, Botvinick E, Liaw L, Sun C-H, Shah J. 2005. Micromanipulation of chromosomes and the mitotic spindle using laser microsurgery (laser scissors) and laser-induced optical forces (laser tweezers). In: Celis J, editor. Cell biology: a laboratory handbook. Burlington, MA: Elsevier Press.

Botvinick EL, Venugopalan V, Shah JV, Liaw LH, Berns MW. 2004. Controlled ablation of microtubules using a picosecond laser. Biophys J 87:4203–4212.

Chumbley LS, Cassucio G, Kritikos D, Lentz H, Mannes C, Mehta K. 2002. Development of a web-based SEM specifically for K-12 education. Microsc Res Tech 56:454–461.

Hadida-Hassan M, Young SJ, Peltier ST, Wong M, Lamont S, Ellisman MH. 1999. Web-based telemicroscopy. J Struct Biol 125: 235–245.

Huang K, Murphy RF. 2004. From quantitative microscopy to automated image understanding. J Biomed Opt 9:893–912.

Kaplan KJ, Burgess JR, Sandberg GD, Myers CP, Bigott TR, Greenspan RB. 2002. Use of robotic telepathology for frozen-section diagnosis: a retrospective trial of a telepathology system for intraoperative consultation. Mod Pathol 15:1197–1204.

McNeill PA, Berns MW. 1981. Chromosome behavior after laser microirradiation of a single kinetochore in mitotic PtK2 cells. J Cell Biol 88:543–553.

Molnar B, Berczi L, Diczhazy C, Tagscherer A, Varga SV, Szende B, Tulassay Z. 2003. Digital slide and virtual microscopy-based routine and telepathology evaluation of routine gastrointestinal biopsy specimens. J Clin Pathol 56:433–438.

Price JH, Goodacre A, Hahn K, Hodgson L, Hunter EA, Krajewski S, Murphy RF, Rabinovich A, Reed JC, Heynen S. 2002. Advances in molecular labeling, high throughput imaging, and machine intelligence portend powerful functional cellular biochemistry tools. J Cell Biochem Suppl 39:194–210.

Takaoka A, Yoshida K, Mori H, Hayashi S, Young SJ, Ellisman MH. 2000. International telemicroscopy with a 3 MV ultrahigh voltage electron microscope. Ultramicroscopy 83:93–101.

Yamada A, Hirahara O, Tsuchida T, Sugano N, Date M. 2003. A practical method for the remote control of the scanning electron microscope. J Electron Microsc (Tokyo) 52:101–109.

Youngblom JH, Youngblom JJ, Wilkinson J. 2001. Telepresence confocal laser scanning microscopy. Microsc Microanal 7:241–248.